

OPEN ACCESS

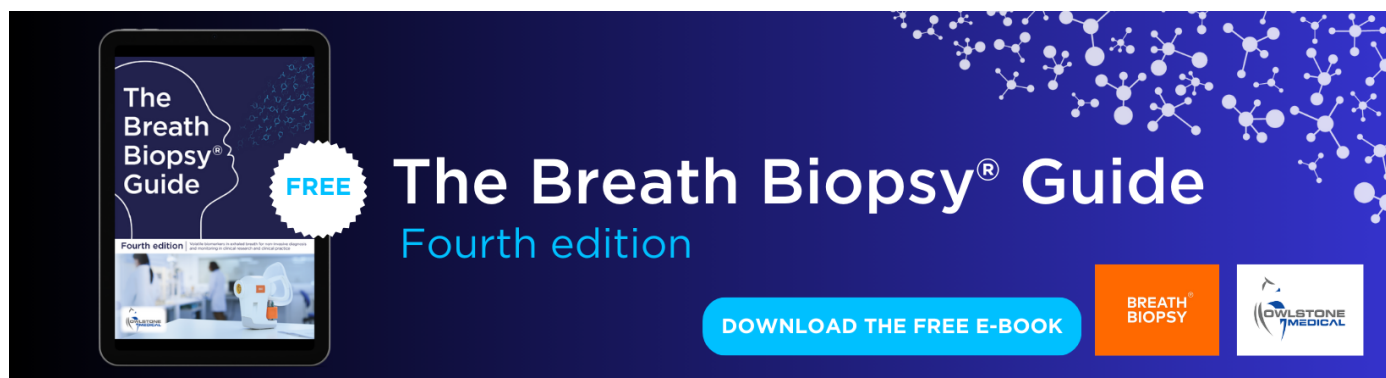
Geoengineering as an optimization problem

To cite this article: George A Ban-Weiss and Ken Caldeira 2010 *Environ. Res. Lett.* **5** 034009

View the [article online](#) for updates and enhancements.

You may also like

- [Characterization of Differently Synthesized Pt-Ru Fuel Cell Catalysts by Cyclic Voltammetry, FTIR Spectroscopy, and in Single Cells](#)
C. Roth, N. Martz, F. Hahn et al.
- [Atmospheric Corrosion of Cu during Constant Deposition of NaCl](#)
Huang Lin and G. S. Frankel
- [Molten Carbonate Fuel Cell Performance for CO₂ Capture from Natural Gas Combined Cycle Flue Gas](#)
Jonathan Rosen, Timothy Geary, Abdelkader Hilmi et al.



The Breath Biopsy® Guide
Fourth edition

FREE

DOWNLOAD THE FREE E-BOOK

BREATH BIOPSY

OWLSTONE MEDICAL

Geoengineering as an optimization problem

George A Ban-Weiss and Ken Caldeira

Department of Global Ecology, Carnegie Institution for Science, 260 Panama Street, Stanford, CA 94305, USA

E-mail: georgebw@stanford.edu

Received 2 July 2010

Accepted for publication 25 August 2010

Published 16 September 2010

Online at stacks.iop.org/ERL/5/034009

Abstract

There is increasing evidence that Earth's climate is currently warming, primarily due to emissions of greenhouse gases from human activities, and Earth has been projected to continue warming throughout this century. Scientists have begun to investigate the potential for geoengineering options for reducing surface temperatures and whether such options could possibly contribute to environmental risk reduction. One proposed method involves deliberately increasing aerosol loading in the stratosphere to scatter additional sunlight to space. Previous modeling studies have attempted to predict the climate consequences of hypothetical aerosol additions to the stratosphere. These studies have shown that this method could potentially reduce surface temperatures, but could not recreate a low-CO₂ climate in a high-CO₂ world. In this study, we attempt to determine the latitudinal distribution of stratospheric aerosols that would most closely achieve a low-CO₂ climate despite high CO₂ levels. Using the NCAR CAM3.1 general circulation model, we find that having a stratospheric aerosol loading in polar regions higher than that in tropical regions leads to a temperature distribution that is more similar to the low-CO₂ climate than that yielded by a globally uniform loading. However, such polar weighting of stratospheric sulfate tends to degrade the degree to which the hydrological cycle is restored, and thus does not markedly contribute to improved recovery of a low-CO₂ climate. In the model, the optimal latitudinally varying aerosol distributions diminished the rms zonal mean land temperature change from a doubling of CO₂ by 94% and the rms zonal mean land precipitation minus evaporation change by 74%. It is important to note that this idealized study represents a first attempt at optimizing the engineering of climate using a general circulation model; uncertainties are high and not all processes that are important in reality are modeled.

Keywords: climate change, geoengineering, global warming, optimization, sulfate aerosol

 Online supplementary data available from stacks.iop.org/ERL/5/034009/mmedia

1. Introduction

Past studies of geoengineering using climate model simulations have taken the approach of imposing a change that affects radiative forcing (e.g., in solar flux, aerosol loading, or aerosol emissions) and then predicting how that imposed change might affect Earth's climate or chemistry. Computations proceed from cause to effect. But, decisions often proceed from desired outcomes to actions that might produce those

outcomes. One approach to thinking about geoengineering is to ask 'What kind of climate do we want?' and then ask 'What pattern of radiative forcing from stratospheric aerosols would come closest to achieving that desired climate state?' This involves treating geoengineering as an optimization problem by defining 'climate goals' and an 'objective function' that measures how closely those goals are attained. An example of a climate goal could be to recreate current surface temperatures in a future high-CO₂ world. An example of an associated

objective function for this climate goal would be to minimize rms differences in the surface temperatures of two simulations. This general approach is developed in the current study.

Global average surface temperatures are estimated to have increased [1] by $0.76 \pm 0.19^\circ\text{C}$ from the period 1850–1899 to 2001–2005. Given the high inertia and long time constants involved in the physical climate system, decreases in emissions of greenhouse gases may be needed soon to avoid future dangerous increases in global temperatures. Despite this serious environmental challenge, emissions have been projected to increase in the future [1]. This has led some to consider whether ‘geoengineering’, defined as ‘the deliberate change of the Earth’s climate by mankind’ [2], might be able to reduce environmental risk. One method of geoengineering that has been discussed is reducing the incident solar radiation to Earth by increasing, for example, sulfate aerosol loading in the stratosphere [3]. Past volcanic eruptions have shown that increased stratospheric aerosol loading can indeed reduce surface temperatures, as illustrated by the 1991 eruption of Mt Pinatubo [4], which injected ~ 10 Mt of sulfur into the stratosphere [5]. However, volcanic eruptions are an ‘imperfect analogy’ to geoengineering because eruptions occur only occasionally, and the radiative forcing from an eruption lasts at most a few years [2].

Many previous studies of the effects on climate of intentionally reducing solar radiation have used global climate models to simply reduce solar insolation [6–11]. These studies investigated climate effects of a globally uniform ‘sunshade’, rather than increasing aerosol loading in the stratosphere. A limited number of studies have investigated the effects of injecting aerosol precursors into the stratosphere at different locations assuming a fixed particle size distribution [12, 13], while another study tracked the evolution of aerosol microphysics in the stratosphere [14]. These studies have concluded that globally reducing incident solar radiation could decrease global mean temperatures, but that, for changes that produce the same global mean temperature decrease, reductions in shortwave radiation produce larger decreases in the hydrological cycle than do reductions in greenhouse gas concentrations [15]. In addition, the spatial climate patterns (e.g. in surface temperature and precipitation) produced by diminished shortwave radiation do not perfectly counter the climate effects of increased CO_2 concentration [11]. Thus, even if it proves possible to cool Earth to the globally averaged surface temperature of some prior climate state, the climate system will not return to that prior climate state [2]. Furthermore, these solar radiation approaches do not reverse ocean acidification, CO_2 -fertilization of land plants, and other biogeochemical changes.

In this letter, we: (1) present the results of five simulations using a global climate model where each simulation uses a different zonal average stratospheric sulfate distribution. These aerosol distributions are described by Legendre polynomials in the sine of latitude (see section 2.2 for more details) and will henceforth be referred to as the ‘basis function’ distributions; (2) investigate the linearity of climate response to different zonal average stratospheric sulfate distributions by performing two additional simulations that use linear combinations of the

basis function distributions; (3) use the results of the previous two steps in an optimization model to predict the zonal average sulfate distributions that would minimize various measures of climate change; (4) perform another set of simulations using these predicted sulfate distributions to see how well our climate goals were achieved. This set of simulations will henceforth be referred to as the ‘forward simulations’.

2. Methods

2.1. Model details

The global climate model used in this study was the NCAR Community Atmosphere Model (CAM3.1) [16] coupled to the Community Land Model (CLM3.0) [17] and a slab ocean model. We used a configuration of CAM3.1 with $2^\circ \times 2.5^\circ$ (longitude \times latitude) resolution and a finite-volume dynamical core. The model approaches a stationary state within 30 years. Results for the last 70 years of each 100-year simulation are presented relative to results from a control simulation with either $\text{CO}_2 = 390$ ppm ($1 \times \text{CO}_2$) or 780 ppm ($2 \times \text{CO}_2$). In this letter we also refer to $1 \times \text{CO}_2$ and $2 \times \text{CO}_2$ as ‘low- CO_2 world’ and ‘high- CO_2 world’, respectively. Concentrations of other greenhouse gases are the same in all simulations.

The CAM3.1 model has 26 layers in the vertical. Each of the basis function simulations increases sulfate aerosol mass by 10 Mt SO_4 (3.3 Mt S) in the top layer of the model (in the stratosphere at ~ 3 mbar ≈ 40 km) and thus zonal average distributions vary but the total mass of added sulfate aerosol remains the same for each simulation; additional sulfate is prescribed and constant (i.e. not advected or time variant). Particle size is assumed to be log-normally distributed with a dry median radius of $0.05 \mu\text{m}$ and geometric standard deviation of 2.0, as was used in a geoengineering scenario in a previous study [12]. The sulfate aerosol does not absorb solar radiation and thus changes in stratospheric circulation are not expected. Aerosol indirect effects are not modeled in this study. Aerosol loadings for species other than sulfates are the same for all simulations. The simulations with additional stratospheric sulfate were carried out with a CO_2 concentration of 780 ppm. All values shown in the figures are zonal averages over land. The simulations carried out in this study, along with their naming conventions and the per cent reductions in net shortwave radiation at the top of atmosphere caused by the aerosol distributions, are summarized in supplementary table S1 (available at stacks.iop.org/ERL/5/034009/mmedia).

2.2. Aerosol distributions

For the basis function simulations, zonal average stratospheric sulfate distributions are represented using Legendre polynomials in the sine of latitude (figure 1). The globally uniform aerosol distribution function is represented by a constant (i.e., a constant times the order zero Legendre polynomial, L_0). The aerosol distribution that linearly increases from the South Pole to North Pole is represented by the sum of a zero and first order (L_1) Legendre polynomial, which is linear in the sine of latitude. The parabolic distribution with a minimum at

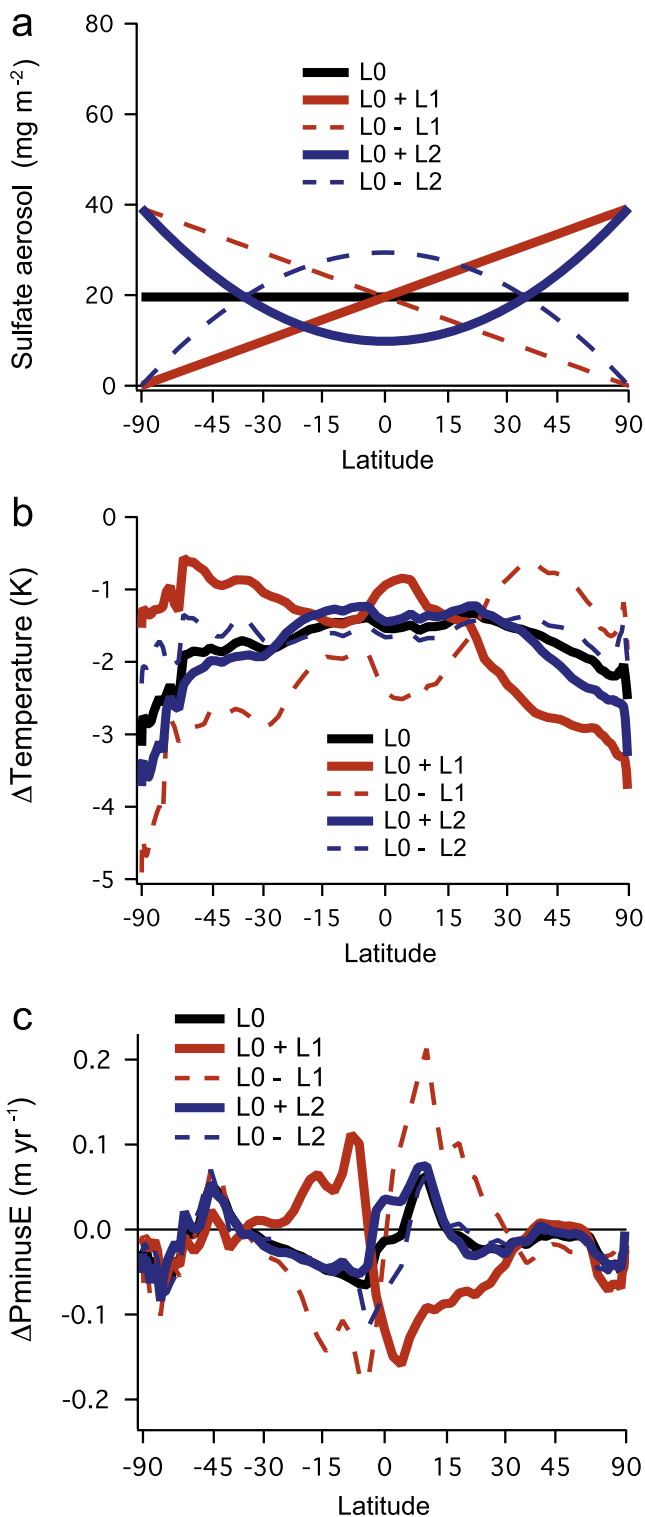


Figure 1. Summary of the ‘basis function’ simulations, where each simulation uses a different zonal average stratospheric sulfate aerosol distribution and a CO₂ concentration of 780 ppm (2 × CO₂). The zonal average aerosol distribution used for each simulation is shown in (a). The resulting zonal average climate response for each simulation is shown in (b) for surface air temperature and (c) for precipitation minus evaporation (PminusE). Both (b) and (c) are averages over land, and are background subtracted using a control simulation with CO₂ = 780 ppm. Results shown are averages of the last 70 years of 100-year simulations.

the equator was represented by the sum of a zero and second order (*L2*) Legendre polynomial. Each of our basis function distributions adds 10 Mt sulfate aerosol, but is distributed latitudinally in different ways. These are idealized distributions used for our theoretical study; we do not address the difficulties involved in creating such distributions in practice.

2.3. Optimization model

Zonal average results over land from the basis function simulations were used in an optimization model to predict the zonal average stratospheric sulfate aerosol distributions most likely to minimize climate change, according to climate goals that we defined. The two climate goals used in this study are: (1) minimize the rms difference in zonal average temperature over land (relative to the 1 × CO₂ climate) in a 2 × CO₂ world; (2) similar to (1) but minimize the rms difference in zonal average precipitation minus evaporation (PminusE). In steady state over land, precipitation in excess of evaporation runs off. These goals were chosen for illustrative purposes only.

The optimization model uses rms difference as the objective function; a linear combination of the basis function distributions were scaled to minimize the rms difference between the 2 × CO₂ climate (with stratospheric aerosols) and the 1 × CO₂ climate. For each climate goal, two distributions were calculated—the first constrained to be a uniform aerosol distribution (i.e., Legendre polynomial of order zero), and the second constrained to be a parabolic distribution in the sine of latitude (i.e., a linear combination of Legendre polynomials up to order two).

3. Results

3.1. Basis function simulations

The simulated responses of surface air temperature and PminusE to the basis function distributions of sulfate aerosol are shown in figure 1. Results are shown relative to a control simulation with 2 × CO₂.

In the case with globally uniform aerosol loading (*L0*), high latitudes cool more than the rest of the globe. This polar amplification has been observed in other climate simulations [1] with different forcing mechanisms such as increased atmospheric CO₂ and has been associated with snow and sea-ice feedbacks. The magnitude of predicted climate system feedbacks would vary with different baseline climates and models. PminusE decreases at most latitudes; the dipole in PminusE change near the equator indicates a northward shift in the intertropical convergence zone (ITCZ).

In the case of aerosol loading increasing linearly from one pole to the other (i.e., *L0 + L1*, *L0 - L1*), latitudes with higher aerosol loading show greater cooling, and latitudes with lower aerosol loading show less cooling; the largest temperature decreases are at the north pole for *L0 + L1* and the south pole for *L0 - L1*. PminusE decreases at most latitudes; the dipole in PminusE change near the equator for *L0 + L1* suggests a southern shift in the ITCZ, whereas *L0 - L1* creates a northward shift that is larger in magnitude than that from the *L0* simulation.

In the case of parabolic aerosol loading with a minimum (i.e., *L0 + L2*) or maximum (i.e., *L0 - L2*) near the equator,

changes in surface air temperature are similar to those of the $L0$ simulation near the equator, but differ at the poles; cooling is enhanced at the poles for the $L0 + L2$ simulation, whereas less cooling is observed at the poles for the $L0 - L2$ simulation. Note that despite the fact that the $L0 - L2$ distribution has no stratospheric sulfate at the poles, a cooling of ~ 2 K is observed at high latitudes, a consequence of atmospheric transport redistributing the effects of the sulfate aerosol. Also note that shifts in ocean circulation might also be expected but we use a slab ocean and thus ocean circulation changes are not modeled. For the $L0 + L2$ and $L0 - L2$ simulations, PminusE is similar to that with a uniform aerosol distribution at most latitudes. The exception is at the equator, where the lower aerosol loading in the $L0 + L2$ simulation relative to the $L0$ simulation (and therefore greater solar energy input) leads to higher values for PminusE. Likewise, the higher equatorial aerosol loading in the $L0 - L2$ simulation (and therefore reduced solar energy input) leads to less PminusE near the equator.

3.2. Assessing the linearity of climate response

In this study we find that the climate response to a linear combination of radiative forcing pattern changes (caused by different stratospheric aerosol distributions) is very similar to the linear combination of the climate responses to radiative forcing pattern changes. Figures 2(a) and (b) each show three different forcing patterns: two distributions used in the basis function simulations, and a linear combination of these two distributions. Figure 2(c) and (d) show the temperature response results from the basis function simulations, the average of these two temperature responses (dashed black line), and temperature response results attained by running additional simulations using the average of the basis function distributions (i.e. the red lines in figures 2(a) and (b)). The fact that the red lines and the dashed black lines in figures 2(c) and (d) are similar shows that the temperature response of the linear combination of the radiative forcing pattern changes, $C[0.5 \times (L0 + L1) + 0.5 \times (L0 + L2)]$ and $C[0.5 \times (L0 - L1) + 0.5 \times (L0 - L2)]$, can be closely approximated by the linear combination of the temperature response to the individual radiative forcing pattern changes, $0.5 \times C[L0 + L1] + 0.5 \times C[L0 + L2]$ and $0.5 \times C[L0 - L1] + 0.5 \times C[L0 - L2]$, where for example $C[L0 + L1]$ represents the climate of the ' $L0 + L1$ ' distribution. Such similarity is also observed for changes in PminusE (figures 2(e) and (f)), though to a lesser extent than temperature. The approximate linearity of climate response to this set of radiative forcing changes provides a means for approximating the pattern of radiative forcing that is likely to most closely produce a specified climate state (section 3.3). In these examples, predicting the climate produced by the mean of two of our basis function distributions based on the mean of the climate response to each distribution taken separately would produce an rms error of 0.08 K (4.0%) in the temperature prediction and 0.007 m yr^{-1} (15.8%) in the PminusE prediction; graphically this is the rms difference between the red and dashed black lines in figures 2(c)–(f), respectively (or this rms difference expressed as the percentage of the rms of the red curve).

3.3. Determination of optimal sulfate distributions for achieving climate goals

Results from the basis function simulations were used in an optimization model (see section 2.3) to predict stratospheric aerosol distributions most likely to achieve two different climate goals. The climate goals we chose are to minimize the change (relative to the $1 \times \text{CO}_2$ climate) in zonal average (1) temperature and (2) PminusE over land in a $2 \times \text{CO}_2$ world. That is, the objectives we chose are to modify climate using stratospheric sulfate aerosol to achieve $1 \times \text{CO}_2$ zonal average land temperatures or PminusE in a $2 \times \text{CO}_2$ world. This choice of objectives is somewhat arbitrary; we chose these objectives as illustrative examples. The resulting idealized zonal distributions of sulfate aerosol were then used in the global climate model with $2 \times \text{CO}_2$ to observe if the predicted latitudinal aerosol distributions would indeed produce the predicted climate, which was intended to be similar to that with $1 \times \text{CO}_2$. In other words, in a $2 \times \text{CO}_2$ world, do our determined sulfate distributions bring climate back to that of a $1 \times \text{CO}_2$ climate, at least in terms of zonal averages? Results for these simulations are shown in figures 3 and 4, which are shown relative to the $1 \times \text{CO}_2$ control simulation.

3.4. Forward simulations—minimizing changes in zonal land mean temperature

The left column of panels in figure 3 shows quantities relevant to the goal of minimizing changes in temperature. Figure 3(a) shows aerosol distributions that are predicted to minimize rms zonal mean temperature change over land (relative to $1 \times \text{CO}_2$) under the constraints of (1) a uniform aerosol distribution and (2) a zonally uniform distribution that can be described by a parabola in the sine of latitude.

When attempting to minimize temperature change, the uniform aerosol distribution ($2 \times \text{CO}_2 + \text{uniform}$) over-cools the tropics and under-cools the poles relative to the $1 \times \text{CO}_2$ control simulation (figure 3(c)); the rms difference in zonal mean surface air temperature between $2 \times \text{CO}_2 + \text{uniform}$ and $1 \times \text{CO}_2$ is 90% lower than the rms difference between $2 \times \text{CO}_2$ and $1 \times \text{CO}_2$ (figure 4(a), supplementary table S2 available at stacks.iop.org/ERL/5/034009/mmedia). The parabolic aerosol distribution ($2 \times \text{CO}_2 + \text{parabolic}$) allows more similarity to the $1 \times \text{CO}_2$ climate with respect to temperature change, as shown in figure 3(c), and reduces the aforementioned rms difference in temperature by 94% (figure 4(a), supplementary table S2 available at stacks.iop.org/ERL/5/034009/mmedia).

In the $2 \times \text{CO}_2$ simulation, PminusE increases in some latitudes and decreases in others (figure 3(e)). The addition of a uniform distribution of sulfate aerosols to the $2 \times \text{CO}_2$ world reduces the rms difference in zonal average PminusE (over land) between the $2 \times \text{CO}_2$ and $1 \times \text{CO}_2$ worlds by 67% (figure 4(b), supplementary table S2 available at stacks.iop.org/ERL/5/034009/mmedia). However, some latitude bands show increases in PminusE, and some show decreases (figure 3(e)). The predicted optimal parabolic distribution leads to a 51% reduction in the rms difference in PminusE (figure 4(b)). Thus, when aerosol loading is increased at high latitudes to decrease the change in zonal mean temperatures (relative to the $1 \times \text{CO}_2$

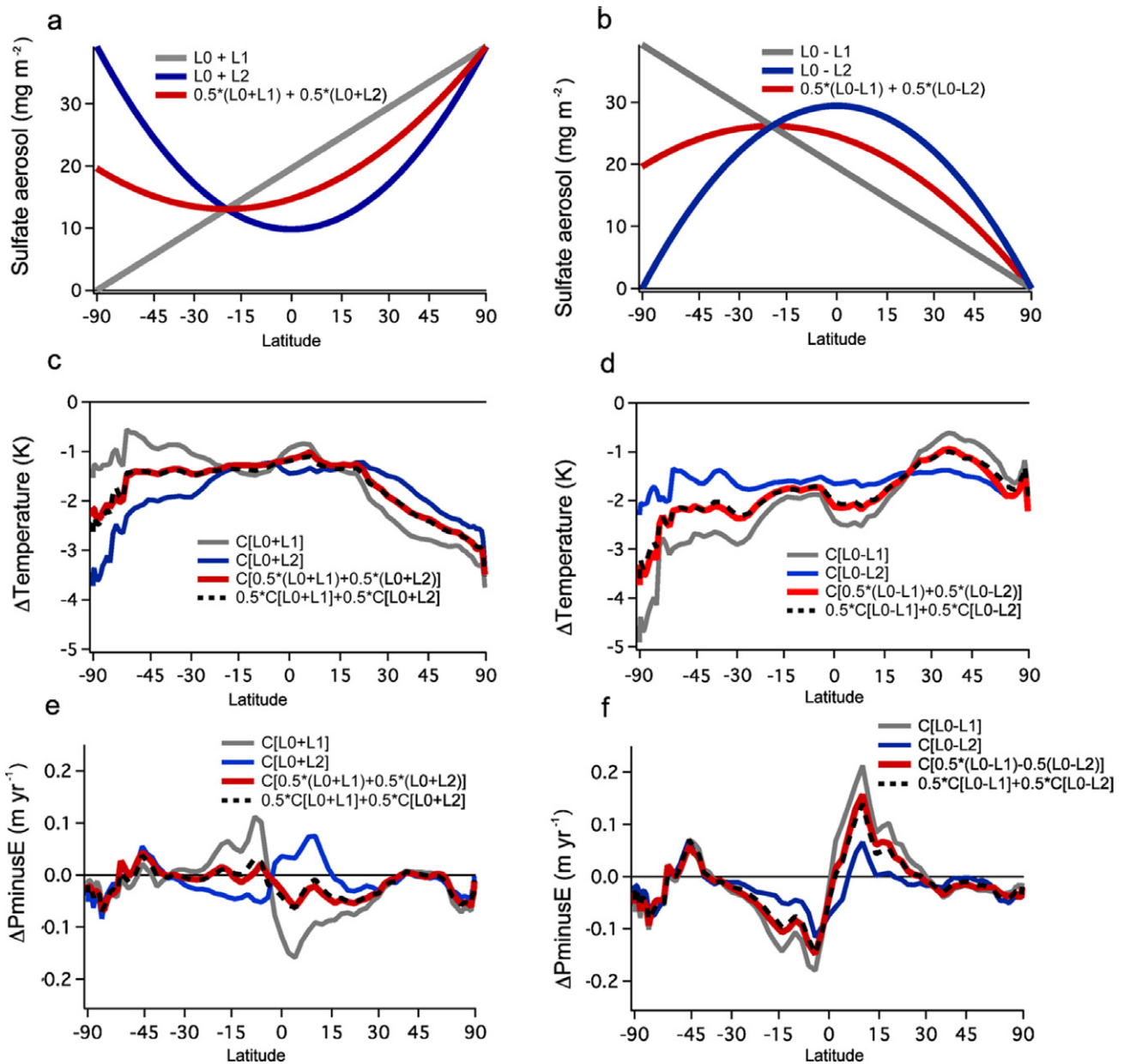


Figure 2. Linearity of climate response to different zonal average stratospheric sulfate aerosol distributions. Panels (a) and (b) show the different zonal average aerosol distributions used in each simulation; note that ‘ $L0 + L1$ ’, ‘ $L0 + L2$ ’, ‘ $L0 - L1$ ’, and ‘ $L0 - L2$ ’ were shown previously in figure 1. The red lines shown in (a) and (b) are linear combinations of the blue and gray lines in each panel, respectively. The resulting zonal average climate response over land for each simulation is shown in (c) and (d) for surface air temperature and (e) and (f) for PminusE. The red lines in (c)–(f) show the climate response of a linear combination of latitudinal aerosol distributions, i.e. red lines in (a) and (b). The dashed black lines in (c)–(f) show the linear combinations of the climate responses, i.e. the gray and blue lines in (c)–(f). The fact that the red and dashed black lines are nearly identical in (c)–(f) shows that the climate response to a linear combination of different latitudinal aerosol distributions is similar to the linear combination of the climate responses of the different zonal aerosol distributions. This suggests that climate response is approximately linear over the range of different latitudinal forcing patterns investigated in this study. Like figure 1, (c)–(f) is background subtracted using a control simulation with $CO_2 = 780$ ppm. Results shown are averages of the last 70 years of 100-year simulations.

climate), there is a reduction in the extent to which PminusE changes are diminished.

3.5. Forward simulations—minimizing changes in zonal land mean PminusE

Figure 3(b) shows the aerosol distributions predicted to minimize changes in PminusE relative to the $1 \times CO_2$ climate. Note that aerosol loadings are less in this case relative to

that of our first climate goal. The ratio of hydrological cycle changes to temperature changes is higher with variations in shortwave radiation than with variations in greenhouse gas concentrations [15], and thus it is expected that optimization on hydrologic variables would yield lower aerosol loadings than would optimization on temperature. Note also that the optimal parabolic aerosol distribution is similar to the uniform distribution. This indicates that, with the constraint of a

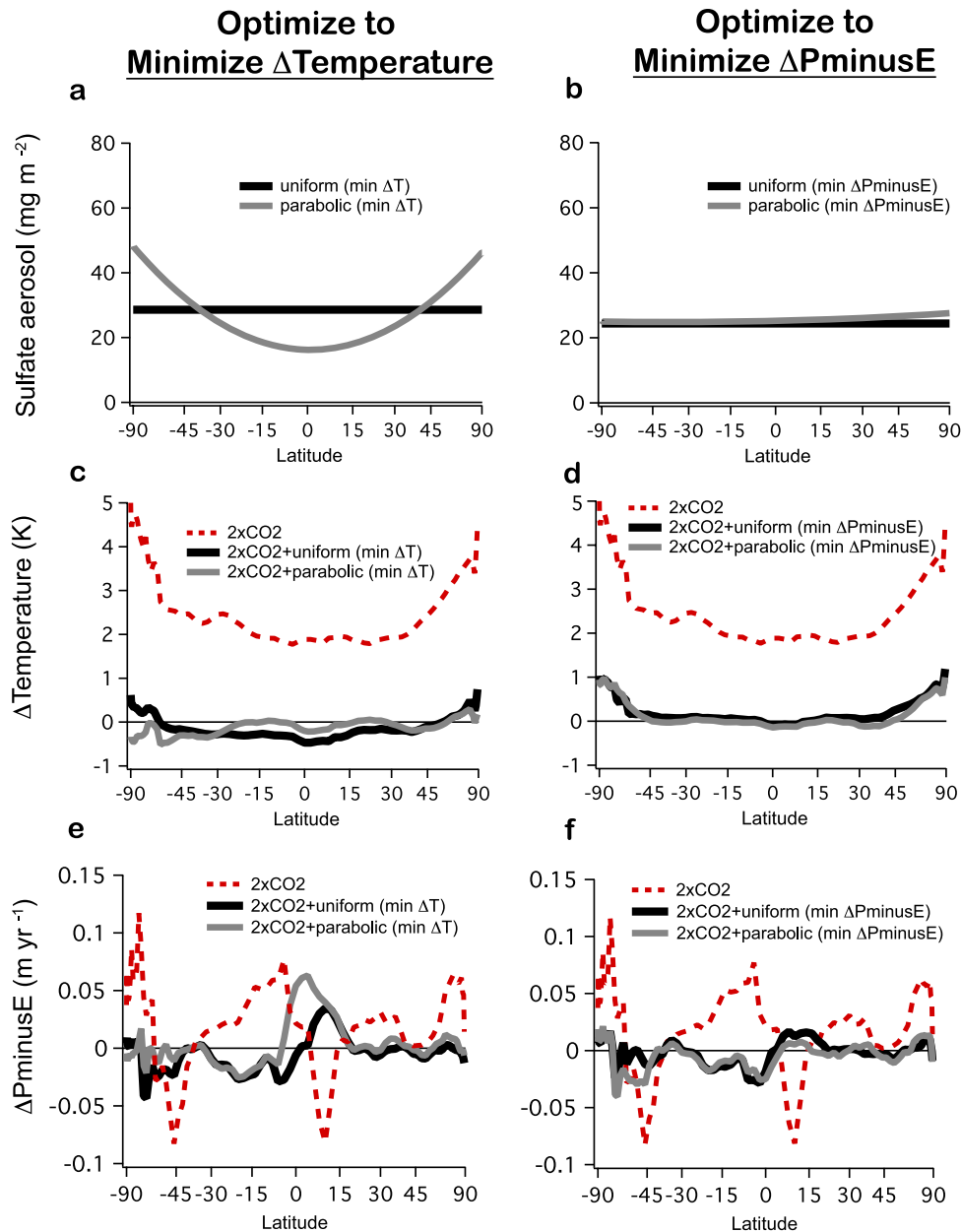


Figure 3. Results of the ‘forward simulations’ using our idealized zonal average stratospheric aerosol distributions that we predicted to be most likely to achieve two different climate goals. The first column shows results for our first goal of regaining the zonal average surface air temperatures over land of the $1 \times \text{CO}_2$ climate in a $2 \times \text{CO}_2$ world. The second column shows results for our second climate goal of regaining the zonal average land PminusE of the $1 \times \text{CO}_2$ climate in a $2 \times \text{CO}_2$ world. We attempt to achieve each climate goal under the constraints of (1) a globally uniform stratospheric aerosol distribution (black lines), and (2) a parabolic distribution in the sine of latitude (gray lines). All simulations use a CO_2 concentration of 780 ppm ($2 \times \text{CO}_2$), and are shown relative to a control simulation with $\text{CO}_2 = 390$ ppm ($1 \times \text{CO}_2$). Results shown are averages over land for surface air temperature ((c), (d)) and PminusE ((e), (f)), and are averages of the last 70 years of 100-year simulations.

time invariant zonal mean aerosol distribution that can be described as a quadratic function of the sine of latitude, there is little improvement in predicted PminusE fields by allowing latitudinally varying aerosol distributions.

Indeed, both the uniform and parabolic aerosol distribution predicted to optimally reduce rms in PminusE in the $2 \times \text{CO}_2$ world relative to the $1 \times \text{CO}_2$ world reduced this rms difference by 74% (figure 4(b), supplementary table S2 available at stacks.iop.org/ERL/5/034009/mmedia). For the reasons stated above, optimizing on hydrological cycle

variables yields lower predicted optimal aerosol loadings and thus larger temperature changes relative to the $1 \times \text{CO}_2$ world (figure 3(d)). The uniform aerosol distribution predicted to optimally reduce rms in PminusE in the $2 \times \text{CO}_2$ world relative to the $1 \times \text{CO}_2$ world reduced the rms difference in temperature by 85%, whereas the parabolic distribution reduced this rms difference in temperature by 87%.

It should be noted that even when the climate goal is to minimize zonal mean changes in PminusE relative to the $1 \times \text{CO}_2$ world, there are zonal bands where changes in

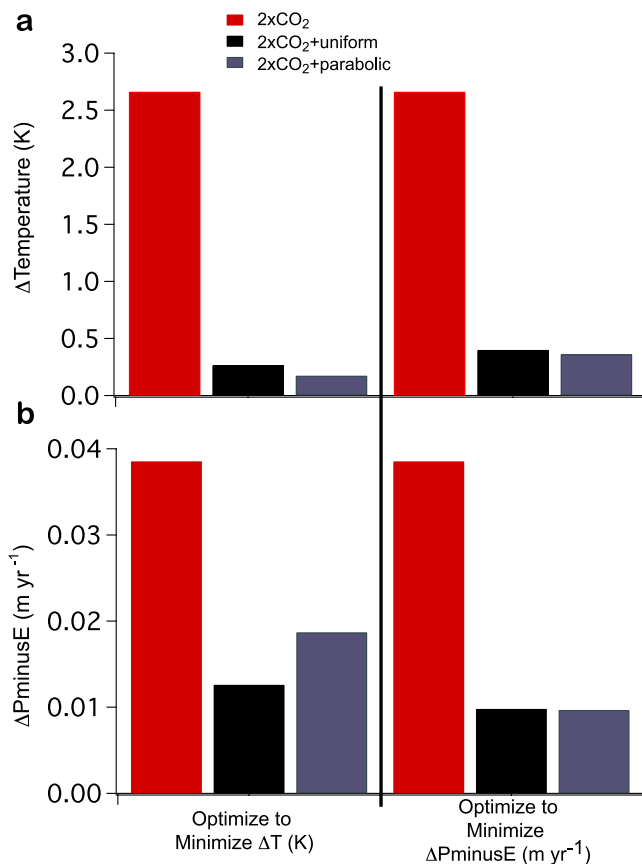


Figure 4. RMS differences of zonal mean land temperature (a) and PminusE (b) between the ‘forward simulations’ with stratospheric aerosols in a $2 \times \text{CO}_2$ world, and a $1 \times \text{CO}_2$ control simulation. The rms differences between the $2 \times \text{CO}_2$ and $1 \times \text{CO}_2$ control simulations are also shown for reference. Lower values for rms difference indicate greater similarity between the $1 \times \text{CO}_2$ climate and the $2 \times \text{CO}_2$ climate with stratospheric aerosols. Numerical values used in this figure are presented in supplementary table S2 (available at stacks.iop.org/ERL/5/034009/mmedia).

PminusE are larger with stratospheric aerosols than in the $2 \times \text{CO}_2$ world (e.g., around 15° North). This raises issues of equity, and suggests that minimizing climate change on the basis of PminusE (or more broadly changes in the hydrological cycle) using sulfate aerosols could be more challenging than minimizing changes in temperature.

3.6. Forward simulations—rms differences computed on each land grid cell

In the previous sections we have analyzed rms differences between the forward simulations and the $1 \times \text{CO}_2$ climate using zonal mean values over land; we presented per cent reductions in the rms differences relative to rms differences between $2 \times \text{CO}_2$ and $1 \times \text{CO}_2$. Since this metric does not take longitudinal changes into account, we also calculated rms differences using all grid cells over land (supplementary table S2 available at stacks.iop.org/ERL/5/034009/mmedia). Reductions in rms difference using zonal land means of surface air temperature are very similar to that using each grid cell over land. This is less true for PminusE because longitudinal shifts occur that do not affect the zonal mean.

For example, for the uniform distribution aimed at minimizing zonal land mean PminusE change, there was an 85.0% and 74.4% reduction in zonal land mean temperature and PminusE change, respectively; for this simulation, there was an 84.0% and 63.9% reduction in temperature and PminusE change, calculated on land-area-weighted grid point by grid point basis (supplementary table S2 available at stacks.iop.org/ERL/5/034009/mmedia).

3.7. Further assessing the linearity of climate response

An additional check of the linearity of climate response to various forcing patterns was performed by comparing the expected climate responses predicted by our optimization model to the actual model responses of the forward simulations. The rms difference between the expected climate response (by taking a linear combination of our basis function distributions) and actual modeled climate response was 0.10 K (3.9%) for surface air temperature and 0.008 m yr^{-1} (18.7%) for PminusE. This is similar to the linearity results previously discussed (section 3.2, figure 2) of 4.0% for temperature response and 15.8% for PminusE.

4. Discussion and conclusions

This letter presents the first attempt to define a climate objective and then predict the stratospheric sulfate aerosol distribution that would best achieve those climate objectives. We first performed five basis function simulations using a global climate model, each of which forced climate with a different latitudinal pattern of stratospheric sulfate aerosol. We then assessed the linearity of surface air temperature and PminusE response to the varying latitudinal forcing patterns. The near-linearity of these results provided a means of creating an optimization model to approximate the pattern of radiative forcing likely to most closely produce a specified climate state. We then defined two (somewhat arbitrary) climate goals and used the optimization model with results of the basis function simulations to predict the latitudinal pattern of stratospheric sulfate aerosol most likely to achieve the climate goals. The predicted stratospheric sulfate aerosol loadings were then used in simulations using the global climate model. Results from these simulations were compared to the climate goals to assess whether they were achieved.

Our model results indicate that optimization approaches can predict distributions of stratospheric aerosols that, in a high- CO_2 world, would make the zonal annual mean climate markedly more similar to that of a low- CO_2 world. With a uniform stratospheric aerosol distribution that restores global mean temperature, there is a tendency to overcool equatorial regions and undercool polar regions. However, if the aerosol is distributed with increased loading closer to the poles so that there is a more nearly uniform offsetting of CO_2 -induced warming, the result is degradation in the offsetting of changes in PminusE. Under the constraints imposed in this study, it does not appear that a latitudinal weighting of aerosol distribution markedly improves the ability to recover the hydrological cycle of a low- CO_2 world in a high- CO_2 world.

Stratospheric aerosol distributions can be optimized to attain similarity to the current climate for surface temperatures, or PminusE (or other measures of the hydrological cycle), but the optimal distributions differ for temperature and PminusE. This is, in part, a consequence of the fact that the hydrological cycle is more sensitive to changes in solar radiation than are surface air temperatures, as reported elsewhere [15]. Furthermore, CO₂ heats up the entire planetary surface and stratospheric aerosols cool the entire planetary surface. In contrast, CO₂ increases PminusE in some places and decreases it in other places. Similarly, stratospheric aerosols have spatially heterogeneous effects on PminusE, but these effects do not closely mirror effects of CO₂ (figure 3). Thus, the ability of sulfate aerosol distributions to offset changes in the hydrological cycle is inherently limited. In the model, the optimal latitudinally varying aerosol distributions diminished the rms zonal mean land temperature change from a doubling of CO₂ by 94% and the rms zonal mean land precipitation minus evaporation change by 74%.

In our study, we prescribe linear and parabolic distributions of aerosol loadings in the stratosphere. We do not consider here whether or how such distributions could be produced. We limit our consideration to aerosol distributions that can be described by a parabola in the sine of latitude (see section 2). Thus we do not consider variation in time or in the longitudinal dimension, nor do we consider distributions in the latitudinal dimension that could be described by higher order polynomials. In this study, we focus on annual-average latitudinal distributions of aerosol, though in general this approach could be extended to include different distributions in both space and time. In addition, we prescribe a fixed particle size distribution. Particle size has been shown to be important in accurately determining climate effects of stratospheric aerosols, but most climate models are not yet able to model the evolution of particle size distribution [12]; the study by Heckendorn *et al* [14] is an exception since they model the evolution of aerosol microphysics. Amounts of sulfate aerosol needed to produce a specific cooling effect are sensitive to particle size.

The climate goals used in this letter were chosen somewhat arbitrarily and were intended to be illustrative. A wide range of possible goals could be explored in future modeling studies. For example, one could attempt to minimize changes in the Asian monsoon, arctic sea ice, extreme weather events, or atmospheric chemistry. It is unknown to what extent such climate goals could be achieved. Though our analysis uses idealized model simulations, in the real world there are serious questions about how such climate goals would be chosen, and what process should be used to make this choice. Future modeling studies could also explore other interventions, including injecting aerosols in different ways, both spatially and temporally (e.g. in different regions and/or seasons) or using aerosols with different optical properties. It is not known to what extent such aerosol injections could be achieved in practice. Future modeling studies could also explore other objective functions such as extending our zonal mean analysis to minimize changes in climate on a grid cell basis. This would account for variability in the longitudinal dimension.

Changes in seasonal or monthly means could be minimized rather than annual means as presented in our study. Further, the optimizations in this study are performed on equilibrium climate simulations, whereas the real world is dynamically changing. Optimizing on transient climate simulations could employ dynamic closed-loop control algorithms.

This study treats geoengineering as an optimization problem. We present idealized results from a global climate model. We focus on scientific results and make no prescriptive statements. However, attempts to intervene in the climate system present a wide range of serious environmental and socio-political risks [2, 18–22], a thorough discussion of which is beyond the scope of this study. Further, the model used here does not include many factors that are important in reality (e.g., socio-political consequences, chemical consequences such as changes in stratospheric ozone, ocean circulation changes, aerosol transport and microphysics). For example, failure to reduce CO₂ emissions will cause oceans to further acidify with potentially catastrophic consequences for ecosystems such as coral reefs [23]. Furthermore, the perception of a technical fix to the climate problem could result in increased emissions with greater long-term environmental damage. Decisions over testing or deployment of climate intervention systems could result in political or military conflict.

The main goal of this letter is to outline a new methodological approach. Previously, researchers have simulated interventions in the climate system and investigated what climate changes would result. Here, we specify climate objectives and investigate what climate interventions would meet those objectives most closely. It is important to note that the climate model used is much simpler than reality and predictions from individual models certainly do not provide a sound basis for action.

References

- [1] IPCC 2007 *Climate Change 2007: The Physical Science Basis. Contribution of Working Group I to the Fourth Assessment Report of the Intergovernmental Panel on Climate Change* ed S Solomon, D Qin, M Manning, Z Chen, M Marquis, K B Averyt, M Tignor and H L Miller (Cambridge & New York: Cambridge University Press) 996 pp
- [2] Rasch P J, Tilmes S, Turco R P, Robock A, Oman L, Chen C C, Stenchikov G L and Garcia R R 2008 An overview of geoengineering of climate using stratospheric sulphate aerosols *Phil. Trans. R. Soc. A* **366** 4007–37
- [3] Crutzen P J 2006 Albedo enhancement by stratospheric sulfur injections: a contribution to resolve a policy dilemma? *Clim. Change* **77** 211–9
- [4] Stenchikov G L, Kirchner I, Robock A, Graf H F, Antuna J C, Grainger R G, Lambert A and Thomason L 1998 Radiative forcing from the 1991 Mount Pinatubo volcanic eruption *J. Geophys. Res. Atmos.* **103** 13837–57
- [5] Bluth G J S, Doiron S D, Schnetzler C C, Krueger A J and Walter L S 1992 Global tracking of the SO₂ clouds from the June, 1991 Mount-Pinatubo eruptions *Geophys. Res. Lett.* **19** 151–4
- [6] Govindasamy B and Caldeira K 2000 Geoengineering Earth's radiation balance to mitigate CO₂-induced climate change *Geophys. Res. Lett.* **27** 2141–4

- [7] Govindasamy B, Thompson S, Duffy P B, Caldeira K and Delire C 2002 Impact of geoengineering schemes on the terrestrial biosphere *Geophys. Res. Lett.* **29** GL015911
- [8] Govindasamy B, Caldeira K and Duffy P B 2003 Geoengineering Earth's radiation balance to mitigate climate change from a quadrupling of CO₂ *Glob. Planet Change* **37** 157–68
- [9] Matthews H D and Caldeira K 2007 Transient climate-carbon simulations of planetary geoengineering *Proc. Natl Acad. Sci. USA* **104** 9949–54
- [10] Caldeira K and Wood L 2008 Global and arctic climate engineering: numerical model studies *Phil. Trans. R. Soc. A* **366** 4039–56
- [11] Lunt D J, Ridgwell A, Valdes P J and Seale A 2008 'Sunshade world': a fully coupled GCM evaluation of the climatic impacts of geoengineering *Geophys. Res. Lett.* **35** L12710
- [12] Rasch P J, Crutzen P J and Coleman D B 2008 Exploring the geoengineering of climate using stratospheric sulfate aerosols: the role of particle size *Geophys. Res. Lett.* **35** L02809
- [13] Robock A, Oman L and Stenchikov G L 2008 Regional climate responses to geoengineering with tropical and arctic SO₂ injections *J. Geophys. Res. Atmos.* **113** D16101
- [14] Heckendorn P, Weisenstein D, Fueglistaler S, Luo B P, Rozanov E, Schraner M, Thomason L W and Peter T 2009 The impact of geoengineering aerosols on stratospheric temperature and ozone *Environ. Res. Lett.* **4** 045108
- [15] Bala G, Duffy P B and Taylor K E 2008 Impact of geoengineering schemes on the global hydrological cycle *Proc. Natl Acad. Sci. USA* **105** 7664–9
- [16] Collins W D *et al* 2004 Description of the NCAR community atmosphere model (CAM 3.0) *NCAR Technical Note NCAR/TN-464 + STR* Natl Cent. Atmos. Res., Boulder, CO
- [17] Oleson K W *et al* 2004 Technical description of the community land model (CLM) *NCAR Technical Note NCAR/TN-461 + STR* Natl Cent. Atmos. Res., Boulder, CO
- [18] Keith D W 2000 Geoengineering the climate: history and prospect *Annu. Rev. Energ. Env.* **25** 245–84
- [19] Robock A 2008 20 reasons why geoengineering may be a bad idea *Atom. Sci. B* **64** 14–8
- [20] Tilmes S, Muller R and Salawitch R 2008 The sensitivity of polar ozone depletion to proposed geoengineering schemes *Science* **320** 1201–4
- [21] Robock A, Marquardt A, Kravitz B and Stenchikov G 2009 Benefits, risks, and costs of stratospheric geoengineering *Geophys. Res. Lett.* **36** L19703
- [22] Tilmes S, Garcia R R, Kinnison D E, Gettelman A and Rasch P J 2009 Impact of geoengineered aerosols on the troposphere and stratosphere *J. Geophys. Res. Atmos.* **114** D12305
- [23] Caldeira K and Wickett M E 2003 Anthropogenic carbon and ocean pH *Nature* **425** 365–5